# DYNAMIC ANALYSIS OF FLEXIBLE MECHANISMS BY FINITE ELEMENT METHOD

**A Thesis Submitted to**
**the Graduate School of Engineering and Sciences of**
**İzmir Institute of Technology**
**in Partial Fulfillment of the Requirements for the Degree of**

**MASTER OF SCIENCE**

**in Mechanical Engineering**

**by**
**Hakan ÜLKER**

**September 2010**
**İZMİR**

We approve the thesis of **Hakan ÜLKER**

**Assoc. Prof. Dr. Bülent YARDIMOĞLU**
Supervisor

**Assist. Prof. Dr. Ebubekir ATAN**
Committee Member

**Assist. Prof. Dr. Aysun BALTACI**
Committee Member

**27 September 2010**

**Prof. Dr. Metin TANOĞLU**
Head of the Department of
Mechanical Engineering

**Assoc. Prof. Dr. Talat YALÇIN**
Dean of the Graduate School
of Engineering and Sciences

# ACKNOWLEDGEMENTS

I would like to thank my advisor Assoc.Prof. Dr. Bülent Yardımoğlu very much for his great help and sharing his very important knowledge and documents about the thesis during this study.

I also would like to thank faculties who tought me engineering courses in both under graduate and graduate levels.

I am delighted to announce that my family has already been with me. I appreciate them for their support during the entire period of my study.

Last but not least I would like to express my deepest gratitude to my wife.

# ABSTRACT


## DYNAMIC ANALYSIS OF FLEXIBLE MECHANISMS BY FINITE ELEMENT METHOD

In this study, vibration characteristics of flexible four-bar mechanisms are investigated by using the procedure developed in ANSYS. Kinematics and kinetics of the four-bar mechanism having rigid and flexible links are presented for finite element modelling of the flexible mechanism. Equations of motion for rigid and flexible four-bar mechanisms are derived by using Lagrangian dynamics to show the theoretical approach. In order to find the natural frequencies of the flexible four-bar mechanism for different configurations, eigenanalysis of the mechanism is carried out by considering the discrete crank positions. Dynamic natural frequencies based on the motion induced axial loads are found by using the discrete inertia forces acting on the nodes of the finite element model. The mode shapes of the flexible four-bar mechanism are also found and plotted with undeformed configurations.

# ÖZET

## ESNEK MEKANİZMALARIN SONLU ELEMANLAR METODU İLE DİNAMİK ANALİZİ

Bu çalışmada, ANSYS'te geliştirilmiş yordam kullanılarak esnek dört çubuk mekanizmalarının titreşim karakteristikleri incelenmiştir. Rijit ve esnek uzuvlu dört çubuk mekanizmalarının kinetik ve kinematik analizleri esnek mekanizmanın sonlu eleman modellenmesi için sunulmuştur. Teorik yaklaşımı göstermek için Lagrange dinamiği kullanılarak rijit ve esnek dört çubuk mekanizmalarının hareket denklemleri elde edilmiştir. Esnek dört çubuk mekanizmasının farklı konumsal durumlarındaki doğal frekansları bulmak için mekanizmanın özdeğer analizi farklı krank pozisyonları düşünülerek gerçekleştirilmiştir. Hareket zorlamalı eksenel yüklere dayanan dinamik doğal frekanslar sonlu elaman modelinin düğümlerine etkiyen farklı atalet kuvvetleri kullanılarak bulunmuştur. Esnek dört çubuk mekanizmasının titreşim biçimleri de bulunmuştur ve şekil değiştirmemiş hali ile birlikte grafiği çizilmiştir.

# TABLE OF CONTENTS

# LIST OF FIGURES

**Figure** **Page**

# LIST OF SYMBOLS

| | |
|---|---|
| $A,B,C$ | quadratic term constants in Equation (2.14) |
| $A_i$ | cross-sectional area of the link i |
| $\vec{a}_i$ | acceleration of link i |
| $a_{px}$ | acceleration of point P in x direction |
| $a_{py}$ | acceleration of point P in y direction |
| $C_1$ | cosine difference |
| $D_1,D_2,D_3,E_1,E_2,E_3$ | link constants |
| $\{\mathrm{d}\}$ | local displacement vector |
| $d_i$ | distance of center of each lumped mass |
| $E_i$ | Young's modulus of link i |
| $\sum F_x$ | total force in x direction in Equation (2.47) |
| $\sum F_y$ | total force in y direction in Equation (2.48) |
| $\vec{F}_i^{inertia}$ | inertial force acting on link i in Equation (2.45) |
| $\mathrm{F_x}$ | total force in Equation (2.84) |
| $G$ | potential energy function defined in Equation (2.62) |
| $G_i$ | lumped mass of link i in Figure 2.2 |
| $g$ | gravitational acceleration |
| $g_i$ | distance of mass center in Figure 2.2 |
| $I$ | area moment of inertia about the bending axis in Equation (2.79) |
| $I_{Gi}$ | mass moment of inertia about centroid for link i |
| $K_1, K_1, K_3$ | link parameters |
| $\left[k^e\right]$ | element stiffness matrix |
| $\left[k_G^e\right]$ | element geometric stiffness matrix |
| $L$ | Lagrangian |
| $L$ | element length in Equation (2.78) |
| $[N]$ | shape functions. |
| M | mass moment of inertia in Equation (2.54) |

| | |
|---|---|
| $\sum M_z$ | total moment in z direction in Equation (2.49) |
| $\vec{M}_i^{inertia}$ | inertial moment of link i in Equation (2.46) |
| $m_i$ | ith mass |
| $\left[m^e\right]$ | element mass matrix |
| $P_i$ | axial force acting on link i |
| $\left\{Q_i^e\right\}$ | generalized forces vector acting on element i |
| $\vec{\mathrm{R}}_{\mathrm{i}}$ | position vector of link i |
| $r_i$ | length of link i in Equation (2.2) |
| $S_i$ | velocity influence coefficient of link i |
| $T_i$ | kinetic energy of link i |
| $T_{ext}$ | driving torque |
| $\left\{\mathrm{u}^{\mathrm{e}}\right\}$ | nodal displacement matrix |
| $V$ | potential energy |
| $V_i$ | strain energy of link i |
| $v_i$ | velocity componentof link i |
| $W_i$ | work potential energy of link i |
| $v_{Gi}$ | center of mass velocity of link i |
| $\mathrm{y}_{\mathrm{Gi}}$ | height of mass center of link i |
| $\alpha_i$ | angular acceleration of link i in Equation (2.25) |
| $\theta_i$ | angles of link i with respect to horizontal axis in Equation (2.2) |
| $\rho$ | mass density |
| $\omega_i$ | angular velocity of link i in Equation (2.19) |
| $\dot{(\ )}$ | derivative with respect to “t” |

# CHAPTER 1

# GENERAL INTRODUCTION

The high productivity, high-technology system demanded by the modern mechanical industry require high operating speeds, superior reliability, accurate performance, light weights and high-precision machinery. In order to overcome high speed operation and increase efficiency, weights of many components in industrial robots and various machines are reduced. As operating speed increases and weights of components decrease, a rigid-body model is not enough anymore. So, these components can not treat as rigid links, they become flexible.

High speed-lightweight manipulators can be thought as an example of flexible multibody system. And four-bar mechanisms are mostly used due to their manufacturing techniques and low cost.

Modeling, analysis and control of flexible mechanisms have been researched since the early 70s. The investigation has been focused mostly on the definition of accurate mathematical models both for single flexible bodies and multi-body systems.

Finite element method is used for modelling of flexible links which behave like both continuous systems with infinite degrees of freedom and discrete systems. A general model to describe the elastic motion of a mechanism can be established with the use of finite element methods resulting in a set of second order differential equations. A common assumption in this procedure is that the total motion is comprised of an elastic motion superposed onto the rigid body motion. As a result the equations of this motion have a significant feature time dependent coefficients. If the effects of nonlinear elastic deflections and/or nonlinear joint characteristics are considered, the equations of motion will be nonlinear. The dynamic response is viewed as a transient response and a steady state response.

A general approach is presented for modelling of a flexible multibody system by using a lumped mass finite element method (Han and Zhao 1990). Modelling and design of controller for a flexible four-bar mechanism is presented. The non-linear equations of motion are obtained by Lagrangian approach (Karkoub and Yigit 1999). Theoretical and practical knowledge of the finite element method and analyzing

engineering problems with ANSYS are studied (Madenci and Guven 2006). Analysis techniques of mechanisms are studied (Söylemez 1999). Deriving the dynamic equation of motion of a four-bar mechanism in order to minimize the dimensions of the mechanism by using Lagrangian formulation is investigated (Tang 2006). Both Freudenstein's equation and the best Chebyshev's theory are studied in order to provide them as best solution for the tasks (Todorov 2002). The equations of motion for a flexible mechanism are obtained by using displacement finite element theory (Turcic and Midha 1984). The method of solution of the equations of motion is the steady-state solution method which allows the steady-state solution (Turcic and Midha 1984). A flexible four-bar mechanism is analyzed to verify the analytical modeling and solution techniques. A comparison of the experimental and analytical results of the mechanism obtained over the specified range is presented (Turcic et al. 1984). Floquet theory for stability analysis of a closed-loop flexible mechanism by using modal coordinates is presented (Yang and Park 1998). The finite element modeling of a flexible mechanism is studied on rigid-elastic coupling and, geometrical stiffness effect of internal axial forces on a beam element (Yang and Sadler 2000). A method for free vibration analysis of planar flexible mechanisms whose body is considered as a beam and modelled using higher-order beam elements for longitudinal and flexural deformations is presented. Dynamical frequencies and dynamical mode shapes including the gyroscopic effects and dynamic axial loads are found by using the modal summation method (Yu and Xi 2003). The geometric nonlinearity due to the large elastic deformations of three flexible links is considered in setting up the dynamic equation of elastic linkages of the mechanism (Yuxin 1997). The first approximation of Liapunov's stability theorem and Floquet theory are used in order to analyze the stability of elastic motion of a flexible four bar crank rocker mechanism (Zhang and Xu 2004).

This thesis has 4 chapters. First chapter presents the subject and summaries the previous studies on the titled subjects. Second chapter provides the theory. Numerical examples and their results are given in Chapter 3. And finally, conclusion is written in Chapter 4.

In this study, natural frequencies and corresponding modes shapes of the flexible mechanisms are investigated by using the procedure developed in ANSYS. The developed procedure uses the discrete crank positions and the discrete inertia forces applied to the nodes of the finite element model. Inertia forces of the links are found by using the kinematic analysis of the rigid four-bar mechanism. Static and dynamic

natural frequencies and corresponding mode shapes are found and presented in graphical forms.

# CHAPTER 2

# ANALYSIS AND MODELLING OF FOUR-BAR MECHANISM

## 2.1. Kinematics of Rigid Four-Bar Mechanism

A four-bar mechanism of which links are drawn as position vectors is shown in Figure 2.1.

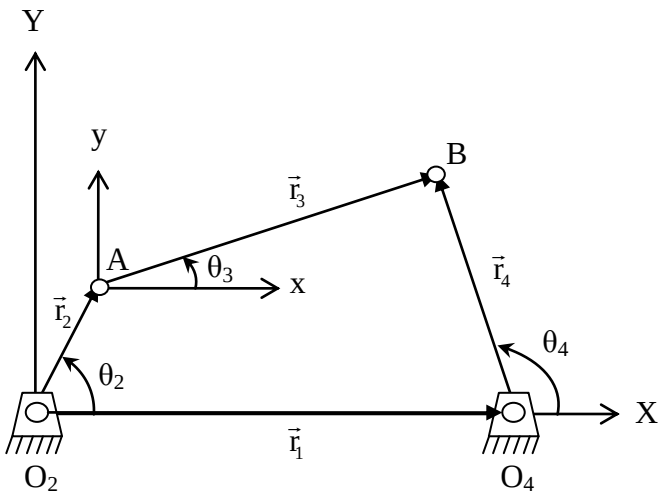


Figure 2.1. A four-bar linkage mechanism showing position vectors

The vector loop closure equation shown in Figure 2.1 is written as:

$$\vec{r}_2 + \vec{r}_3 - \vec{r}_4 - \vec{r}_1 = 0 \tag{2.1}$$

Equation 2.1 is expressed in terms of complex numbers as follows:

$$r_2 e^{i\theta_2} + r_3 e^{i\theta_3} - r_4 e^{i\theta_4} - r_1 = 0 \tag{2.2}$$

By using the Euler expansion, Equation 2.2 is written as:

$$\begin{aligned} r_2(\cos\theta_2 + i\sin\theta_2) + r_3(\cos\theta_3 + i\sin\theta_3) \\ - r_4(\cos\theta_4 + i\sin\theta_4) - r_1 = 0 \end{aligned} \tag{2.3}$$

Equation 2.3 can be resolved into real and imaginary parts as:

$$r_2\cos\theta_2 + r_3\cos\theta_3 - r_4\cos\theta_4 - r_1 = 0 \tag{2.4}$$

$$r_2\sin\theta_2 + r_3\sin\theta_3 - r_4\sin\theta_4 = 0 \tag{2.5}$$

Taking the square of both sides of Equations 2.4 and 2.5 and summing them, the following equation is found:

$$r_3^{\,2} = (-r_2\sin\theta_2 + r_4\sin\theta_4)^2 + (-r_2\cos\theta_2 + r_4\cos\theta_4 + r_1)^2 \tag{2.6.a}$$

and by arranging:

$$\begin{aligned} r_3^{\,2} = r_2^{\,2} + r_4^{\,2} + r_1^{\,2} - 2r_2r_1\cos\theta_2 + 2r_4r_1\cos\theta_4 \\ - 2r_2r_4(\sin\theta_2\sin\theta_4 + \cos\theta_2\cos\theta_4) \end{aligned} \tag{2.6.b}$$

is obtained. To simplify the Equation 2.6.b, the constants $K_1$, $K_2$, and $K_3$ are defined in terms of the constant link lengths in the equations:

$$K_1 = \frac{r_1}{r_2} \tag{2.7}$$

$$K_2 = \frac{r_1}{r_4} \tag{2.8}$$

$$K_3 = \frac{r_2^{\,2} - r_3^{\,2} + r_4^{\,2} + r_1^{\,2}}{2r_2r_4} \tag{2.9}$$

$$K_1\cos\theta_4 - K_2\cos\theta_2 + K_3 = \cos\theta_2\cos\theta_4 + \sin\theta_2\sin\theta_4 \tag{2.10}$$

Then Freudenstein's equation (Todorov 2002) is obtained as follows:

$$\mathrm{K}_1 \cos\theta_4 - \mathrm{K}_2 \cos\theta_2 + \mathrm{K}_3 = \cos(\theta_2 - \theta_4) \tag{2.11}$$

In order to reduce the Equation 2.11 to a more tractable form for solution, the following half angle identities are substituted:

$$\sin\theta_4 = \frac{2\tan(\frac{\theta_4}{2})}{1+\tan^2(\frac{\theta_4}{2})} \tag{2.12}$$

$$\cos\theta_4 = \frac{1-\tan^2(\frac{\theta_4}{2})}{1+\tan^2(\frac{\theta_4}{2})} \tag{2.13}$$

Then, the following equation which is quadratic in terms of $\tan(\theta_4/2)$ is found:

$$A\tan^2(\frac{\theta_4}{2}) + B\tan(\frac{\theta_4}{2}) + C = 0 \tag{2.14}$$

where

$$A = \cos\theta_2 - \mathrm{K}_1 \cos\theta_2 - \mathrm{K}_2 \cos\theta_2 + \mathrm{K}_3 \tag{2.15}$$

$$B = -2\sin\theta_2 \tag{2.16}$$

$$C = \mathrm{K}_1 - (\mathrm{K}_2 + 1)\cos\theta_2 + \mathrm{K}_3 \tag{2.17}$$

$\theta_4$ expressed in Equation 2.14 can be found by solving the quadratic equation as:

$$\theta_4 = 2\tan^{-1}(\frac{-B \pm \sqrt{B^2 - 4AC}}{2A}) \tag{2.18}$$

where the plus and minus sign refers to two different configuration of the mechanism.

In order to make velocity analysis of four-bar linkage, the derivation of Equation 2.2 is considered since $r_1$ is constant and $\omega_1 = 0$, the aformentioned equation is found:

$$ir_2\omega_2 e^{i\theta_2} + ir_3\omega_3 e^{i\theta_3} - ir_4\omega_4 e^{i\theta_4} = 0 \tag{2.19}$$

Resolving into real and imaginary parts, the following equations are written:

$$r_2\omega_2 \cos\theta_2 + r_3\omega_3 \cos\theta_3 - r_4\omega_4 \cos\theta_4 = 0 \tag{2.20}$$

and

$$-r_2\omega_2 \sin\theta_2 - r_3\omega_3 \sin\theta_3 + r_4\omega_4 \sin\theta_4 = 0 \tag{2.21}$$

Then velocity equations are obtained as follows:

$$\omega_3 = \frac{r_2\omega_2}{r_3}\frac{\sin(\theta_4 - \theta_2)}{\sin(\theta_3 - \theta_4)} \tag{2.22}$$

$$\omega_4 = \frac{r_2\omega_2}{r_4}\frac{\sin(\theta_2 - \theta_3)}{\sin(\theta_4 - \theta_3)} \tag{2.23}$$

In order to make acceleration analysis of four-bar linkage, the derivation of Equation 2.19 is taken and the following equation is found:

$$\begin{aligned} &-r_2\omega_2^2 e^{i\theta_2} + ir_2\alpha_2 e^{i\theta_2} - r_3\omega_3^2 e^{i\theta_3} \\ &+ ir_3\alpha_3 e^{i\theta_3} + r_4\omega_4^2 e^{i\theta_4} - ir_4\alpha_4 e^{i\theta_4} = 0 \end{aligned} \tag{2.24}$$

Resolving into real and imaginary parts, the following equations are written:

$$\begin{aligned} &-r_2\omega_2^2 \cos\theta_2 - r_2\alpha_2 \sin\theta_2 - r_3\omega_3^2 \cos\theta_3 \\ &- r_3\alpha_3 \sin\theta_3 + r_4\omega_4^2 \cos\theta_4 + r_4\alpha_4 \sin\theta_4 = 0 \end{aligned} \tag{2.25}$$

and

$$\begin{aligned} &- r_2\omega_2^{\,2}\sin\theta_2 + r_2\alpha_2\cos\theta_2 - r_3\omega_3^{\,2}\sin\theta_3 \\ &+ r_3\alpha_3\cos\theta_3 + r_4\omega_4^{\,2}\sin\theta_4 - r_4\alpha_4\cos\theta_4 = 0 \end{aligned} \tag{2.26}$$

The following parameters are defined:

$$D_1 = -r_2\omega_2^{\,2}\cos\theta_2 - r_2\alpha_2\sin\theta_2 - r_3\omega_3^{\,2}\cos\theta_3 + r_4\omega_4^{\,2}\cos\theta_4 \tag{2.27}$$

$$D_2 = -r_3\sin\theta_3 \tag{2.28}$$

$$D_3 = r_4\sin\theta_4 \tag{2.29}$$

$$E_1 = -r_2\omega_2^{\,2}\sin\theta_2 + r_2\alpha_2\cos\theta_2 - r_3\omega_3^{\,2}\sin\theta_3 + r_4\omega_4^{\,2}\sin\theta_4 \tag{2.30}$$

$$E_2 = r_3\cos\theta_3 \tag{2.31}$$

$$E_3 = -r_4\cos\theta_4 \tag{2.32}$$

Therefore, Equation 2.25 and 2.26 are written as:

$$D_1 + D_2\alpha_3 + D_3\alpha_4 = 0 \tag{2.33}$$

$$E_1 + E_2\alpha_3 + E_3\alpha_4 = 0 \tag{2.34}$$

Then, acceleration equations are obtained as follows:

$$\alpha_3 = \frac{-D_1E_3 + D_3E_1}{D_2E_3 - E_2D_3} \tag{2.35}$$

$$\alpha_4 = \frac{-E_1D_2 + E_2D_1}{D_2E_3 - E_2D_3} \tag{2.36}$$

By carrying out the substitution and simplification, angular acceleration expressions of link 3 and link 4 are found as (Söylemez 1999):

$$\alpha_3 = \frac{r_2\omega_2^{\,2}\cos(\theta_2-\theta_4) + r_2\alpha_2\sin(\theta_2-\theta_4) + r_3\omega_3^{\,2}\cos(\theta_4-\theta_3) - r_4\omega_4^{\,2}}{r_3\sin(\theta_4-\theta_3)} \tag{2.37}$$

$$\alpha_4 = \frac{r_2\omega_2^{\,2}\cos(\theta_2-\theta_3) + r_2\alpha_2\sin(\theta_2-\theta_4) - r_4\omega_4^{\,2}\cos(\theta_4-\theta_3) + r_3\omega_3^{\,2}}{r_4\sin(\theta_4-\theta_3)} \tag{2.38}$$

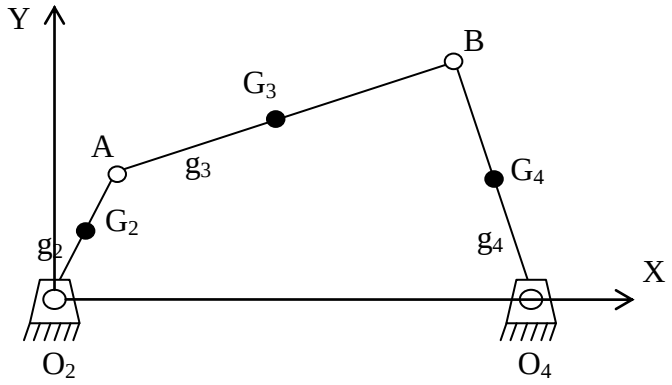


Figure 2.2. Four-bar mechanism showing the centers of gravity of links

The centers of gravity of the links are shown in Figure 2.2. Accelerations of the centers of gravity can be found using the standard kinematic relationships as follows:

$$a_{G2x} = -g_2\omega_2^{\,2}\cos\theta_2 - g_2\alpha_2\sin\theta_2 \tag{2.39}$$

$$a_{G2y} = -g_2\omega_2^{\,2}\sin\theta_2 + g_2\alpha_2\cos\theta_2 \tag{2.40}$$

$$a_{G3x} = -r_2\omega_2^{\,2}\cos\theta_2 - r_2\alpha_2\sin\theta_2 - g_3\omega_3^{\,2}\cos\theta_3 - g_3\alpha_3\sin\theta_3 \tag{2.41}$$

$$a_{G3y} = -r_2\omega_2^{\,2}\sin\theta_2 + r_2\alpha_2\cos\theta_2 - g_3\omega_3^{\,2}\sin\theta_3 + g_3\alpha_3\cos\theta_3 \tag{2.42}$$

$$a_{G4x} = -g_4\omega_4^{\,2}\cos\theta_4 - g_4\alpha_4\sin\theta_4 \tag{2.43}$$

$$a_{G4y} = -g_4\omega_4^{\,2}\sin\theta_4 + g_4\alpha_4\cos\theta_4 \tag{2.44}$$

## 2.2. Kinetics of Rigid Four-Bar Mechanism

Kinetic analysis of rigid four-bar mechanism is based on the accelerations of the centers of gravity given by Equations 2.39 to 2.44.

Inertial force and inertial moment of the link i are given by

$$\vec{F}_i^{\,inertia} = -m_i\vec{a}_i \tag{2.45}$$

$$\vec{M}_i^{\,inertia} = -I_{Gi}\vec{\alpha}_i \tag{2.46}$$

It is well-known that inertial force and inertial moment represent the resistence to linear and angular accelerations, respectively.

For dynamic force analysis of four-bar mechanism under external force or/and moment, dynamic equilibrium conditions for any link i are given as:

$$\sum F_x = \sum m_i a_{ix} \tag{2.47}$$

$$\sum F_y = \sum m_i a_{iy} \tag{2.48}$$

$$\sum M_z = \sum I_{Gi}\alpha_i \tag{2.49}$$

Considering the dynamic equilibrium conditions for each link, the unknown forces can be found using the standard procedure which are available in related textbooks.

## 2.3. Equations of Motion

Lagrangian dynamic formulation is employed to derive equation of motion of rigid and flexible four-bar mechanism.

### 2.3.1. Lagrangian Method for Rigid Four-Bar Mechanism

The four-bar mechanism shown in Figure 2.2 is considered again. The total kinetic energy of the mechanism is written below:

$$T = \frac{1}{2}\sum_{i=1}^{3}(m_i v_{Gi}^2 + I_{Gi}\omega_i^2) \tag{2.50}$$

Then the total potential energy of the system is written as follows:

$$\mathrm{V} = \mathrm{m}_2 g \mathrm{y}_{\mathrm{G2}} + \mathrm{m}_3 g \mathrm{y}_{\mathrm{G3}} + \mathrm{m}_4 g \mathrm{y}_{\mathrm{G4}} \tag{2.51}$$

The Lagrangian of the entire system can be written as:

$$L = T - V \tag{2.52}$$

Since the four-bar mechanism has one degree of freedom, all parameters can be written in terms of $\theta_2$. Therefore, the equation of motion by using Lagrange equation can be expressed as:

$$\frac{d}{dt}\left(\frac{\partial L}{\partial \omega_2}\right) - \frac{\partial L}{\partial \theta_2} = T_{ext} \tag{2.53}$$

It can be found in compact form as (Tang 2006):

$$M(\theta_2)\alpha_2 + V(\theta_2, \omega_2) = T_{\theta 2} \tag{2.54}$$

where

$$M(\theta_2) = 2\left[J_2 + J_3 S_2^2 + J_4 S_3^2 + P_2 C_1 S_2\right] \tag{2.55}$$

$$V(\theta_2,\omega_2)=\begin{bmatrix} 2J_3S_2\left(\frac{\partial S_2}{\partial\theta_2}+S_2\frac{\partial S_2}{\partial\theta_3}+S_3\frac{\partial S_2}{\partial\theta_4}\right) \\ +2J_4S_3\left(\frac{\partial S_3}{\partial\theta_2}+S_2\frac{\partial S_3}{\partial\theta_3}+S_3\frac{\partial S_3}{\partial\theta_4}\right) \\ +P_2C_1\left(\frac{\partial S_2}{\partial\theta_2}+S_2\frac{\partial S_2}{\partial\theta_3}+S_3\frac{\partial S_2}{\partial\theta_4}\right) \\ +P_2S_2\left(\frac{\partial C_1}{\partial\theta_2}+S_2\frac{\partial C_1}{\partial\theta_3}\right) \\ -\frac{\partial G}{\partial\theta_2}-S_2\frac{\partial G}{\partial\theta_3}-S_3\frac{\partial G}{\partial\theta_4} \end{bmatrix}\omega_2 \tag{2.56}$$

in which

$$J_2=\frac{1}{2}(m_2g_2^2+I_{G2}+m_3r_2^2) \tag{2.57}$$

$$J_3=\frac{1}{2}(m_3g_3^2+I_{G3}) \tag{2.58}$$

$$J_4=\frac{1}{2}(m_4g_4^2+I_{G4}) \tag{2.59}$$

$$P_2=m_3r_2g_3 \tag{2.60}$$

$$C_1(\theta_2,\theta_3)=\cos(\theta_2-\theta_3) \tag{2.61}$$

$$G(\theta_2,\theta_3,\theta_4)=(-\mathrm{m}_2gg_2-\mathrm{m}_3gr_2)\sin\theta_2-\mathrm{m}_3gg_3\sin\theta_3-\mathrm{m}_4gg_4\sin\theta_4 \tag{2.62}$$

$$S_2(\theta_2,\theta_3,\theta_4)=\frac{\partial\theta_3}{\partial\theta_2}=\frac{r_2\sin(\theta_4-\theta_2)}{r_3\sin(\theta_3-\theta_4)} \tag{2.63}$$

$$S_3(\theta_2,\theta_3,\theta_4)=\frac{\partial\theta_4}{\partial\theta_2}=\frac{r_2\sin(\theta_3-\theta_2)}{r_4\sin(\theta_3-\theta_4)} \tag{2.64}$$

## 2.3.2. Lagrangian Method for Flexible Four-Bar Mechanism

The deformed and undeformed configuration of flexible four-bar mechanism is shown in Figure 2.3 (Yu and Xi 2003).

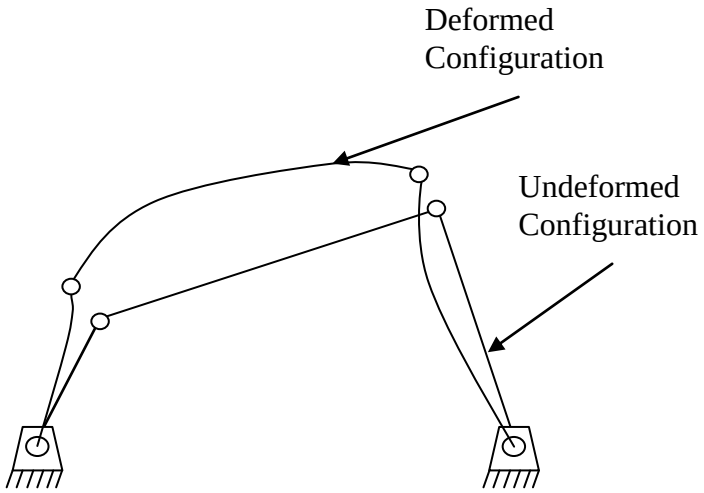


Figure 2.3. Deformed and undeformed configurations of flexible four-bar mechanism.

The position of any arbitrary point P on any link j shown in Figure 2.4 is written in the body-fixed coordinate system xoy as (Yu and Xi 2003):

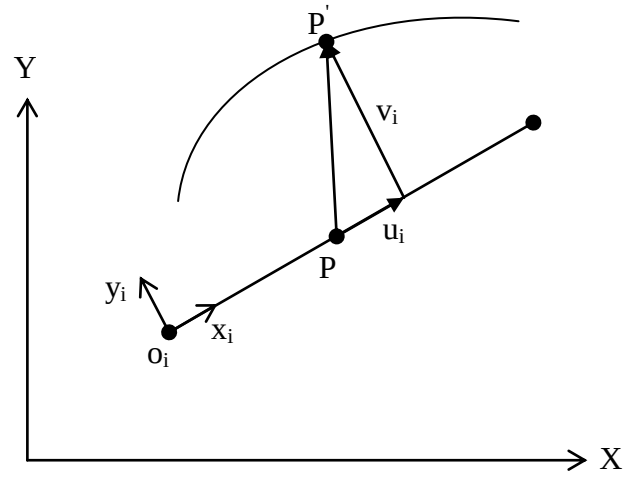


Figure 2.4. Displacement of any arbitrary point P.

$$\vec{R}_i = \vec{R}_{0,i} + \begin{Bmatrix} \vec{e}_{x,i} & \vec{e}_{y,i} \end{Bmatrix} \begin{Bmatrix} x_i + u_i \\ v_i \end{Bmatrix} \tag{2.65}$$

where $\vec{R}_{0,i}$ is the rigid-body position vector of reference point $o_i$, $\vec{e}_{x,i}$, and $\vec{e}_{y,i}$ are unit vectors in the $x_i$ and $y_i$ directions, respectively.

The absolute velocity of point P'can be written in body-fixed coordinate system as follows:

$$\dot{\vec{R}}_i = \begin{Bmatrix} v_{o,i,x} \\ v_{o,i,y} \end{Bmatrix} + \begin{Bmatrix} -\omega_i v_i \\ \omega_i (x_i + u_i) \end{Bmatrix} \begin{Bmatrix} \dot{u}_i \\ \dot{v}_i \end{Bmatrix} \tag{2.66}$$

where $v_{o,i,x}$ and $v_{o,i,y}$ are the x and y velocity components of the reference point $o_i$. $\dot{u}_i$ and $\dot{v}_i$ are the time derivatives of lateral and longitudinal deflections.

The kinetic energy of the link i is given by:

$$T_i = \frac{1}{2}\int_0^{r_i} \rho_i A_i \dot{\vec{R}}_i \dot{\vec{R}}_i dx_i \tag{2.67}$$

The strain energy of the link i is given by:

$$V_i = \frac{1}{2}\int_0^{r_i} E_i A_i \left(\frac{\partial u}{\partial x_i}\right)^2 dx_i + \frac{1}{2}\int_0^{r_i} E_i I_i \left(\frac{\partial^2 v}{\partial x^2{}_i}\right) dx_i \tag{2.68}$$

The work potential of the axial force for any link i is given by:

$$W_i = \frac{1}{2}\int_0^{r_i} P_i \left(\frac{\partial v}{\partial x_i}\right)^2 dx_i \tag{2.69}$$

where $P_i$ is the axial force acting on the link i.

The lagrangian for link i may be written as:

$$L_i = T_i - V_i - W_i \tag{2.70}$$

Depending on the selected generalized coordinate, equation of motion is found. For example, using the finite element discretization technique, equation of motion for flexible mechanism can be found. This is given in next section.

## 2.4. Finite Element Model for Flexible Four-Bar Mechanism

The finite element model shown in Figure 2.5 is used to model any link of the flexible four-bar mechanism (Turcic and Midha 1984).

$$\{d\} = [N]\{u^e\} \tag{2.71}$$

where $\{d\}$ is the local displacement vector of any point on element and $\{u^e\}$ is the nodal displacements vector including nodal displacements shown in Figure 2.5.

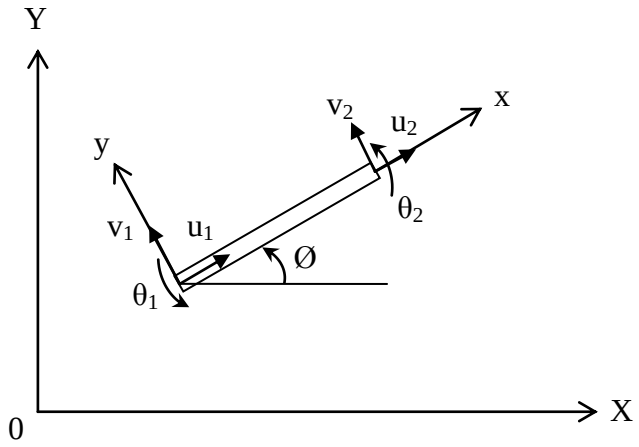


Figure 2.5. A finite element for flexible link

$$\{u^e\} = [u_1 \quad v_1 \quad \theta_1 \quad u_2 \quad v_2 \quad \theta_2]^T \tag{2.72}$$

The equation of motion for a single finite element of the mechanism is derived by using Lagrangian equation:

$$\frac{d}{dt}\left(\frac{\partial KE}{\partial\{\dot{u}^e\}}\right)-\frac{\partial(KE)}{\partial\{u^e\}}+\frac{\partial(PE)}{\partial\{u^e\}}=\{Q\} \tag{2.73}$$

where $\{Q\}$ are the generalized forces acting on elements.

The position of any point in the finite element $\{R\}$ shown in figüre 2.6 can be written as:

$$\{R\}=\{R_0\}+[T_m]\{d\} \tag{2.74}$$

where $\{R_0\}$ is the position of the origin of the local (x,y) coordinate system, $[T_m]$ is the transformation matrix between the local (x,y) coordinate system and the reference (X,Y) coordinate system which is given by:

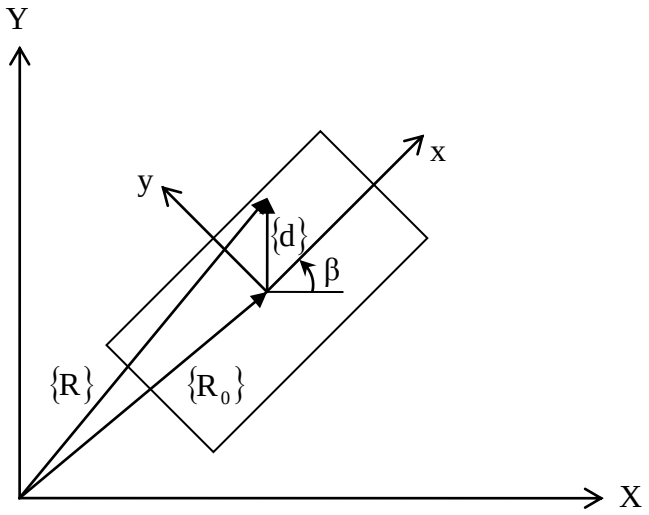


Figure 2.6. Positions of any point in terms of $\{d\}$

$$[T_m]=\begin{bmatrix}\cos\theta & -\sin\theta\\ \sin\theta & \cos\theta\end{bmatrix} \tag{2.75}$$

The kinetic energy of the element is given below:

$$KE=\frac{1}{2}\int\rho\{\dot{R}\}^T\{\dot{R}\}dV \tag{2.76}$$

The equation of motion of a single finite element is expressed as:

$$\left[m^e\right]\left\{\ddot{\mathrm{u}}^{\mathrm{e}}\right\}+\left[k^e\right]\left\{\mathrm{u}^{\mathrm{e}}\right\}=\left\{\mathrm{Q}_{\mathrm{e1}}^{\mathrm{e}}\right\}+\left\{\mathrm{Q}_1^{\mathrm{e}}\right\}+\left\{\mathrm{Q}_{\mathrm{ex}}^{\mathrm{e}}\right\}-\left[m^e\right]\left\{\ddot{\mathrm{U}}_0^{\mathrm{e}}\right\}-2\left[m_{vel}^e\right]\left\{\dot{\mathrm{u}}^{\mathrm{e}}\right\}-\left[m_{acc}^e\right]\left\{\mathrm{u}^{\mathrm{e}}\right\} \quad (2.77)$$

where

$$\left[m^e\right]=\rho AL\begin{bmatrix} 1/3 & 0 & 0 & 1/6 & 0 & 0 \\ 0 & 13/35 & 11L/210 & 0 & 9/70 & -13L/420 \\ 0 & 11L/210 & L^2/105 & 0 & 13L/420 & -L^2/140 \\ 1/6 & 0 & 0 & 1/3 & 0 & 0 \\ 0 & 9/70 & 13L/420 & 0 & 13/35 & -11L/210 \\ 0 & -13L/420 & -L^2/140 & 0 & -11L/210 & L^2/105 \end{bmatrix} \quad (2.78)$$

$$\left[k^e\right]=\begin{bmatrix} EA_x/L & 0 & 0 & -EA_x/L & 0 & 0 \\ 0 & 12EI/L^3 & 6EI/L^2 & 0 & -12EI/L^3 & 6EI/L^2 \\ 0 & 6EI/L^2 & 4EI/L & 0 & -6EI/L^2 & -2EI/L \\ -EA_x/L & 0 & 0 & EA_x/L & 0 & 0 \\ 0 & -12EI/L^3 & -6EI/L^2 & 0 & 12EI/L^3 & -6EI/L^2 \\ 0 & 6EI/L^2 & 2EI/L & 0 & -6EI/L^2 & 4EI/L \end{bmatrix} \quad (2.79)$$

$$\left[m_{vel}^e\right]=\int\rho\left[N\right]^T\left[T_m\right]^T\left[\dot{T}_m\right]\left[N\right]dV \quad (2.80)$$

$$\left[m_{acc}^e\right]=\int\rho\left[N\right]^T\left[T_m\right]^T\left[\ddot{T}_m\right]\left[N\right]dV \quad (2.81)$$

$\left\{\mathrm{Q}_{\mathrm{e1}}^{\mathrm{e}}\right\}$ is the force vector having the forces acting on the elements from adjacent elements, $\left\{\mathrm{Q}_1^{\mathrm{e}}\right\}$ is the force vector due to the adjacent links, $\left\{\mathrm{Q}_{\mathrm{ex}}^{\mathrm{e}}\right\}$ is the external force vector acting on the element. $2\left[m_{vel}^e\right]\left\{\dot{\mathrm{u}}^{\mathrm{e}}\right\}$ has the forces resulting from Coriolis acceleration and $\left[m_{acc}^e\right]\left\{\mathrm{u}^{\mathrm{e}}\right\}$ has the forces resulting from tangential and normal accelerations.

The equation of motion of links is expressed as (Turcic and Midha 1984):

$$\left[m^l\right]\left\{\ddot{\mathrm{u}}^{\mathrm{l}}\right\}+\left[k^l\right]\left\{\mathrm{u}^{\mathrm{l}}\right\}=\left\{\mathrm{Q}_1^{\mathrm{l}}\right\}+\left\{\mathrm{Q}_{\mathrm{ex}}^{\mathrm{l}}\right\}-\left[m^l\right]\left\{\ddot{\mathrm{U}}_0^{\mathrm{l}}\right\}-2\left[m_{vel}^l\right]\left\{\dot{\mathrm{u}}^{\mathrm{l}}\right\}-\left[m_{acc}^l\right]\left\{\mathrm{u}^{\mathrm{l}}\right\} \quad (2.82)$$

The equation of motion of entire mechanism is given by (Turcic and Midha 1984):

$$\begin{aligned}&[M]\{\ddot{u}\}+[C]\{\ddot{u}\}+[K]\{u\}=\{Q_{ex}\}-[M]\{\ddot{U}_0\}-2[[Md+M_{vel}]]\{\dot{u}\}\\&-[[Mdd+2Md_{vel}+M_{acc}]]\{u\}\end{aligned} \tag{2.83}$$

where $[C]$ is the viscous damping matrix, $\{u\}$ is the displacement vector, $\{\dot{u}\}$ is the velocity vector, $\{\ddot{u}\}$ is the acceleration vector, and $\{\ddot{U}_0\}$ is the rigid body acceleration vector of the mechanism.

The derivation of equation of motion is based on small strain theory. However axial force is effective of the stiffness properties of the beam. Using the large strain theory, the geometric stiffness matrix is found as follows (Turcic and Midha 1984):

$$[k_G^e]=\frac{F}{L}\begin{bmatrix}0&0&0&0&0&0\\0&6/5&L/10&0&-6/5&L/10\\0&L/10&2L^2/15&0&-L/10&-L^2/30\\0&0&0&0&0&0\\0&-6/5&-L/10&0&6/5&-L/10\\0&L/10&-L^2/30&0&-L/10&2L^2/15\end{bmatrix} \tag{2.84}$$

where F is axial force acting on element.

The equation of motion given by Equation 2.83 has been modified as (Yang and Sadler 2000):

$$[M]\{\ddot{U}\}+([C_0]+2[M_\omega])\{\dot{U}\}+([K_0]+[M_\alpha])\{U\}=\{F\}-[M]\{\ddot{U}_0\} \tag{2.85}$$

where

$$[M_\omega]_i=[\tilde{T}]_i^T\left(\int\rho_i A_i[N]_i^T[T_2]_i[\dot{T}_2]_i^T[N]_i\,dx\right)[\tilde{T}]_i \tag{2.86}$$

and

$$[M_\alpha]_i=[\tilde{T}]_i^T\left(\int\rho_i A_i[N]_i^T[T_2]_i[\ddot{T}_2]_i^T[N]_i\,dx\right)[\tilde{T}]_i \tag{2.87}$$

Eigenanalysis is applied to the system having mass and structural stiffness matrices, due to lack of generalized force vector in free vibration analysis as follows (Yu and Xi 2003):

$$[M_r(\theta_2)]\{\ddot{U}_r\}+[K_r(\theta_2)]\{U_r\}=0 \tag{2.88}$$

From the following equation the natural frequencies and modal vectors can be obtained for flexible four-bar mechanism:

$$[K_r(\theta_{2,k})]\{X\}=\omega_n^2[M_r(\theta_{2,k})]\{X\} \tag{2.89}$$

# CHAPTER 3

# NUMERICAL EXAMPLES

## 3.1. Introduction

In this chapter, two example flexible mechanisms are presented for different loading conditions. The first one is selected for free vibration analysis of flexible four bar mechanism with different crank angles. In the second example, inertia forces are considered to find the natural frequencies of the flexible four bar mechanism for different configurations. The developed procedure in ANSYS is tested by using the results available in the literature, then some applications are done.

## 3.2. Kinetics of Four-Bar Mechanism

In this section, kinetic analysis of an example for four-bar mechanism is presented for rigid and flexible models. Flexible four-bar mechanism is modelled by using beam finite elements in ANSYS. The following subsections gives the details for the solution procedure developed in this study.

### 3.2.1. Rigid Mechanism

Figure 3.1 shows an example for four-bar mechanism modelled by using lamped parameter approach. The inertia forces given by Equation 2.42 for the lumped masses can be found by using the acceleration expressions given by Equations 2.36 to 2.41. Considering these forces, kinetic analysis of rigid four-bar mechanism can be carried out by using the standard procedure based on the Equation 2.44 to 2.46.

The inertia forces acting on these lumped masses are summarized below:

$$F_{ix} = -m_i a_{ix} \qquad i = 1,...,12 \tag{3.1}$$

$$F_{iy} = -m_i a_{iy} \qquad i = 1,...,12 \qquad (3.2)$$

where $a_i$ is the acceleration of mass $m_i$ and can be calculated by using the formulation given in Equations 2.36 to 2.41.

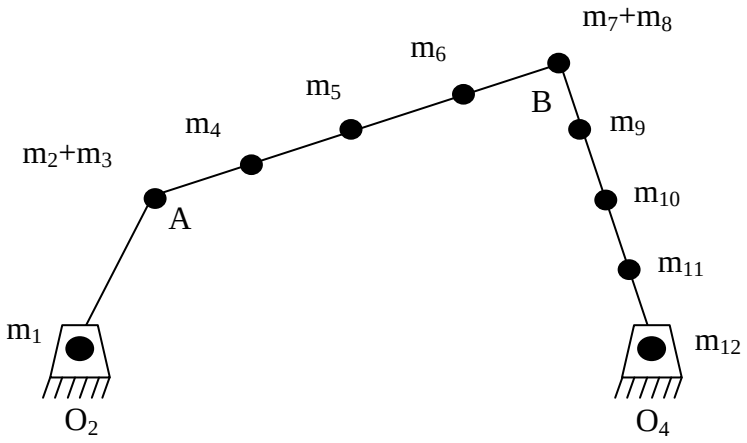


Figure 3.1. A four-bar mechanism showing lumped masses.

The numerical values of the first mechanism shown in Figure 3.1 are listed below:

$r_1 = 254mm$ (length of link 1)

$r_2 = 100mm$ (length of link 2)

$r_3 = 279.4mm$ (length of link 3)

$r_4 = 266.7mm$ (length of link 4)

$d_4 = 69.85mm$ (distance between $A$ and $m_4$)

$d_5 = 139.7mm$ (distance between $A$ and $m_5$)

$d_6 = 209.55mm$ (distance between $A$ and $m_6$)

$d_9 = 200.025mm$ (distance between $O_4$ and $m_9$)

$d_{10} = 133.35mm$ (distance between $O_4$ and $m_{10}$)

$d_{11} = 66.675mm$ (distance between $O_4$ and $m_{11}$)

In the second mechanism, the numerical values are taken as the same listed above except $r_2$=102 *mm*.

For the four-bar mechanism shown in Figure 3.1, the acceleration of the lumped masses are:

$$a_{2x} = a_{3x} = -r_2\omega_2^{\,2}\cos\theta_2 - r_2\alpha_2\sin\theta_2 \tag{3.3}$$

$$a_{2y} = a_{3y} = -r_2\omega_2^{\,2}\sin\theta_2 + r_2\alpha_2\cos\theta_2 \tag{3.4}$$

$$a_{4x} = -r_2\omega_2^{\,2}\cos\theta_2 - r_2\alpha_2\sin\theta_2 - d_4\omega_3^{\,2}\cos\theta_3 - d_4\alpha_3\sin\theta_3 \tag{3.5}$$

$$a_{4y} = -r_2\omega_2^{\,2}\sin\theta_2 + r_2\alpha_2\cos\theta_2 - d_4\omega_3^{\,2}\sin\theta_3 + d_4\alpha_3\cos\theta_3 \tag{3.6}$$

$$a_{5x} = -r_2\omega_2^{\,2}\cos\theta_2 - r_2\alpha_2\sin\theta_2 - d_5\omega_3^{\,2}\cos\theta_3 - d_5\alpha_3\sin\theta_3 \tag{3.7}$$

$$a_{5y} = -r_2\omega_2^{\,2}\sin\theta_2 + r_2\alpha_2\cos\theta_2 - d_5\omega_3^{\,2}\sin\theta_3 + d_5\alpha_3\cos\theta_3 \tag{3.8}$$

$$a_{6x} = -r_2\omega_2^{\,2}\cos\theta_2 - r_2\alpha_2\sin\theta_2 - d_6\omega_3^{\,2}\cos\theta_3 - d_6\alpha_3\sin\theta_3 \tag{3.9}$$

$$a_{6y} = -r_2\omega_2^{\,2}\sin\theta_2 + r_2\alpha_2\cos\theta_2 - d_6\omega_3^{\,2}\sin\theta_3 + d_6\alpha_3\cos\theta_3 \tag{3.10}$$

$$a_{7x} = a_{8x} = -r_2\omega_2^{\,2}\cos\theta_2 - r_2\alpha_2\sin\theta_2 - d_7\omega_3^{\,2}\cos\theta_3 - d_7\alpha_3\sin\theta_3 \tag{3.11}$$

$$a_{7y} = a_{8y} = -r_2\omega_2^{\,2}\sin\theta_2 + r_2\alpha_2\cos\theta_2 - d_7\omega_3^{\,2}\sin\theta_3 + d_7\alpha_3\cos\theta_3 \tag{3.12}$$

$$a_{9x} = -d_9\omega_4^{\,2}\cos\theta_4 - d_9\alpha_4\sin\theta_4 \tag{3.13}$$

$$a_{9y} = -d_9\omega_4^{\,2}\sin\theta_4 + d_9\alpha_4\cos\theta_4 \tag{3.14}$$

$$a_{10x} = -d_{10}\omega_4^{\,2}\cos\theta_4 - d_{10}\alpha_4\sin\theta_4 \tag{3.15}$$

$$a_{10y} = -d_{10}\omega_4^{\,2}\sin\theta_4 + d_{10}\alpha_4\cos\theta_4 \tag{3.16}$$

$$a_{11x} = -d_{11}\omega_4^{\,2}\cos\theta_4 - d_{11}\alpha_4\sin\theta_4 \tag{3.17}$$

$$a_{11y} = -d_{11}\omega_4^{\,2}\sin\theta_4 + d_{11}\alpha_4\cos\theta_4 \tag{3.18}$$

### 3.2.2. Flexible Mechanism

The flexible four-bar mechanism selected as an example earlier modelled by BEAM4 and COMBIN7 elements in ANSYS (Madenci and Guven 2006). The finite element model is shown in Figure 3.2. Element numbers are shown in square boxes.

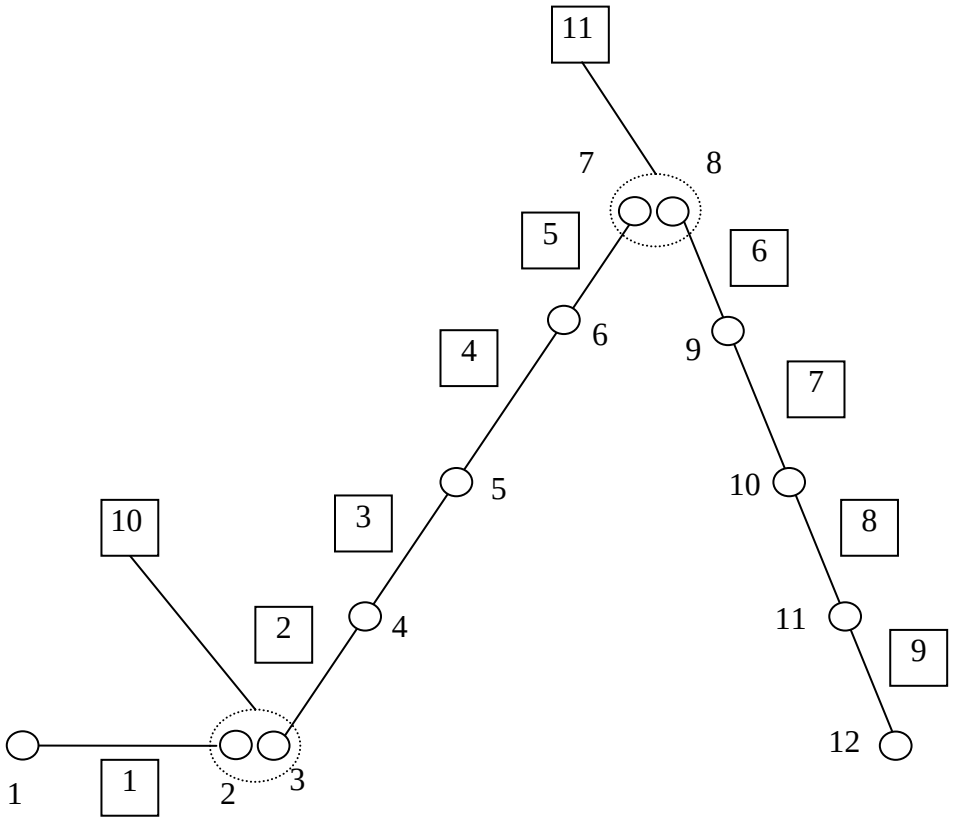


Figure 3.2. Finite element model of flexible four-bar mechanism.

The cross-sectional dimensions and material properties of the first flexible four-bar mechanism are listed below (Yu and Xi 2003):

| | |
|---|---|
| $b = 1.6\,mm$ | (width of the links) |
| $h = 25.4mm$ | (height of the links) |
| $\mathrm{E} = 200000\ \ MPa$ | (modulus of elasticity) |
| $\rho = 7.8*10^{-9}\ \ tonnes/mm^3$ | (density) |
| $\nu = 0.3$ | (poisson's ratio) |

For the second mechanism, the cross-sectional dimensions and material properties are given as (Yu and Xi 2003):

| | |
|---|---|
| $b_2 = 4.24\,mm$ | (width of the link2) |
| $h_2 = 25.4mm$ | (height of the link2) |
| $b_3 = 1.6\,mm$ | (width of the link3) |
| $h_3 = 25.4mm$ | (height of the link3) |
| $b_4 = 1.6\,mm$ | (width of the link4) |
| $h_4 = 25.4mm$ | (height of the link4) |
| $\mathrm{E} = 68900\ \ MPa$ | (modulus of elasticity) |
| $\rho_2 = 2.698*10^{-9}\ \ tonnes/mm^3$ | (density of link2) |
| $\rho_3 = 2.923*10^{-9}\ \ tonnes/mm^3$ | (density of link3) |
| $\rho_4 = 2.923*10^{-9}\ \ tonnes/mm^3$ | (density of link4) |
| $\nu = 0.3$ | (poisson's ratio) |

The boundary conditions of the mechanism are applied as:

- Node 1 is clamped due to the input torque applied to link 2.
- Node 12 is pinned.

## 3.3. Vibrations of the Flexible Mechanism

### 3.3.1. Natural Frequencies of Mechanism without Internal Force

Natural frequencies of flexible four-bar mechanism modelled by finite element method are found in ANSYS for different crank angle $\theta_2$. This type analysis is known as eigenanalysis of mechanism for instantaneous structure. For the mechanism of which parameters are given in previous sections, the natural frequencies and corresponding mode shapes are presented in Figures 3.3 to 3.12.

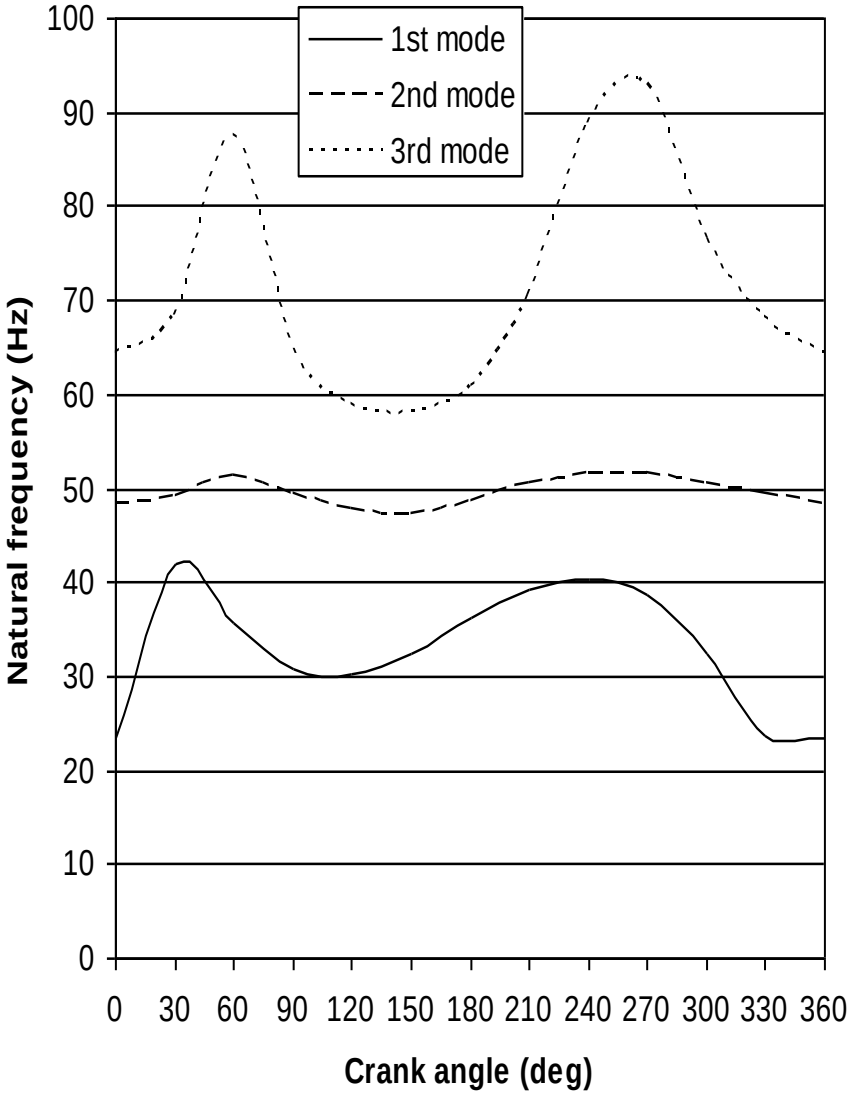


Figure 3.3. Natural frequencies of flexible four-bar mechanism.

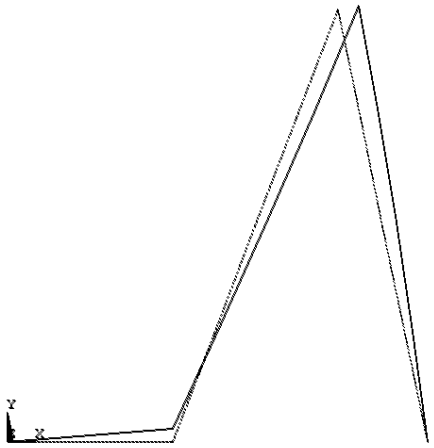

Figure 3.4. First mode shape of flexible four-bar mechanism for $\theta_2=0^o$.

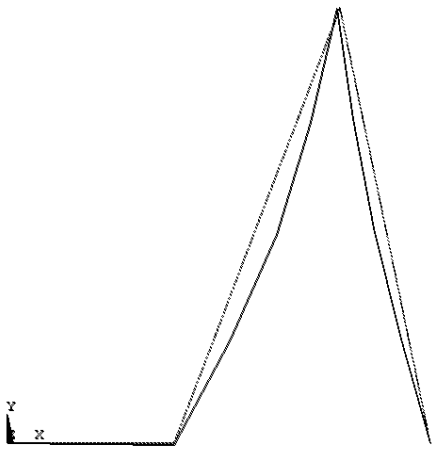

Figure 3.5. Second mode shape of flexible four-bar mechanism for $\theta_2=0^o$.

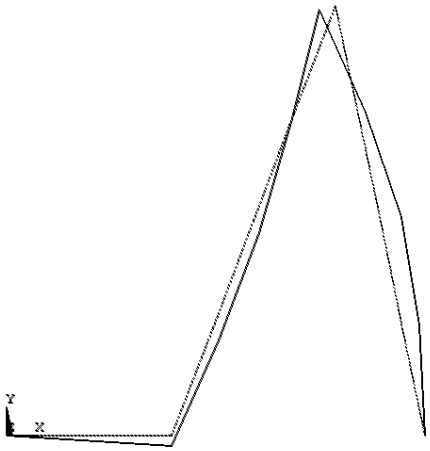

Figure 3.6. Third mode shape of flexible four-bar mechanism for $\theta_2=0^o$.

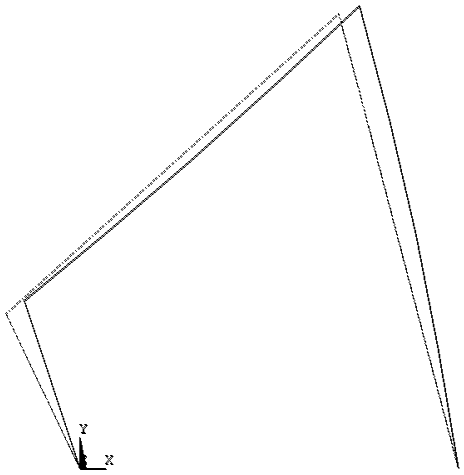


Figure 3.7. First mode shape of flexible four-bar mechanism for $\theta_2=120^o$.

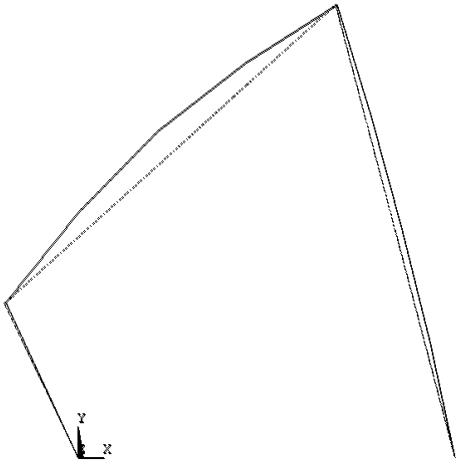


Figure 3.8. Second mode shape of flexible four-bar mechanism for $\theta_2=120^o$.

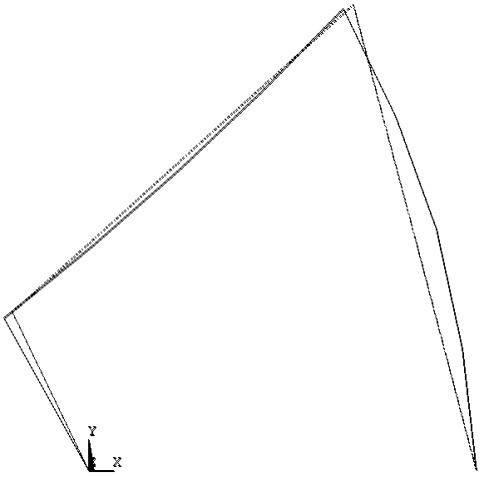


Figure 3.9. Third mode shape of flexible four-bar mechanism for $\theta_2=120^o$.

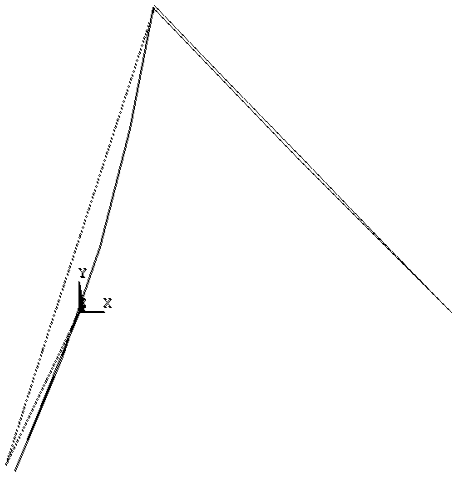


Figure 3.10. First mode shape of flexible four-bar mechanism for $\theta_2=240^o$.

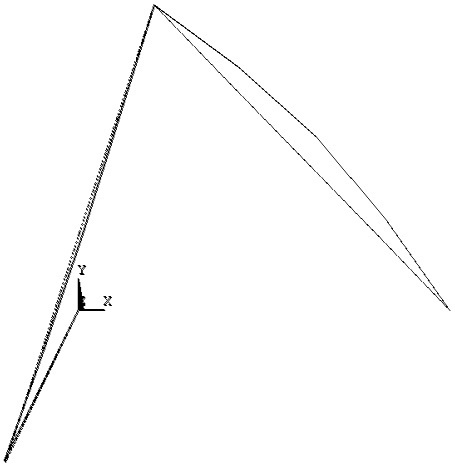


Figure 3.11. Second mode shape of flexible four-bar mechanism for $\theta_2=240^o$.

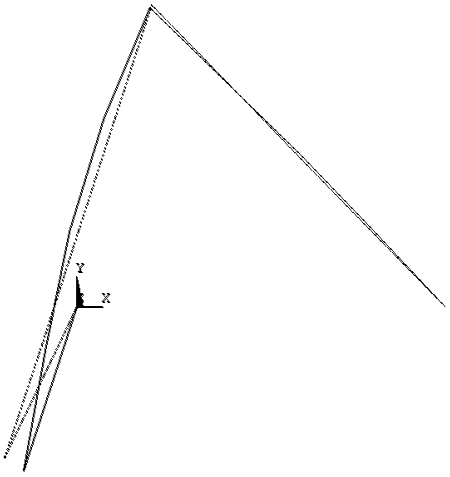


Figure 3.12. Third mode shape of flexible four-bar mechanism for $\theta_2=240^o$.

### 3.3.2. Natural Frequencies of Mechanism with Internal Force

The internal force due to the inertia force are taken into account in finding the natural frequencies of mechanism for different angular velocities $\omega_2$. Inertia forces acting on the lumped masses of the mechanism are considered in finite element model created in Ansys. The results are shown in Figures 3.13 to 3.21.

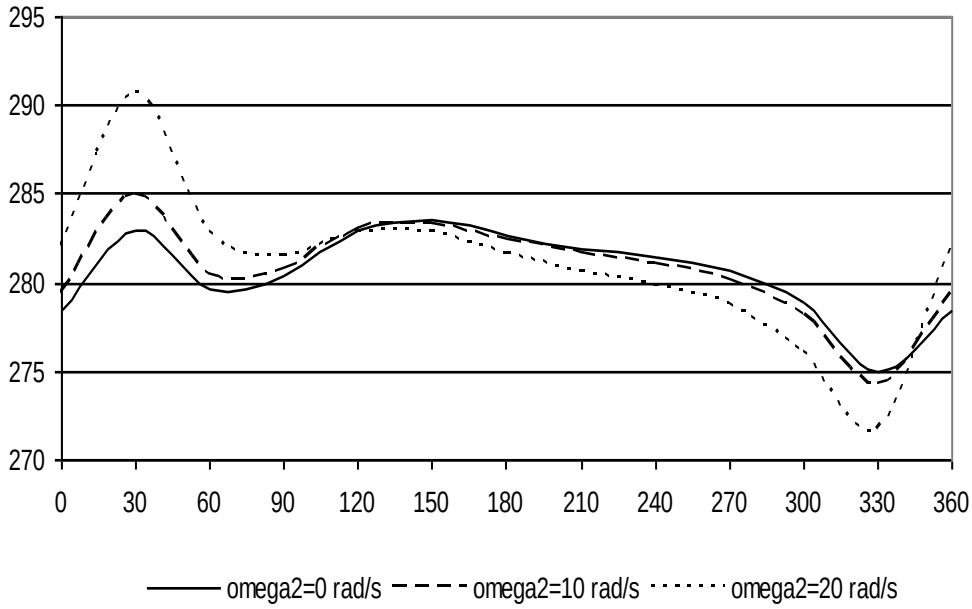


Figure 3.13. First natural frequencies of flexible four-bar mechanism.

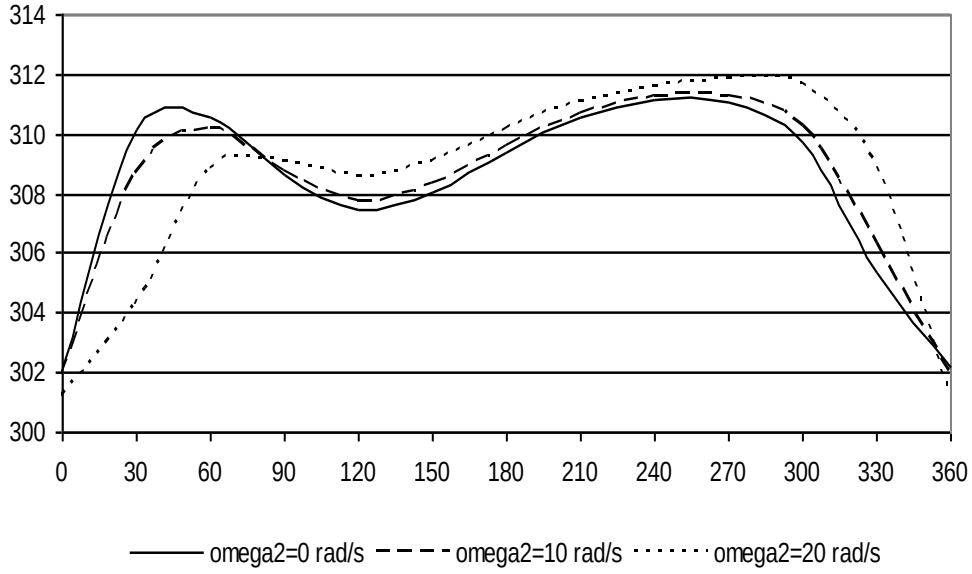


Figure 3.14. Second natural frequencies of flexible mechanism.

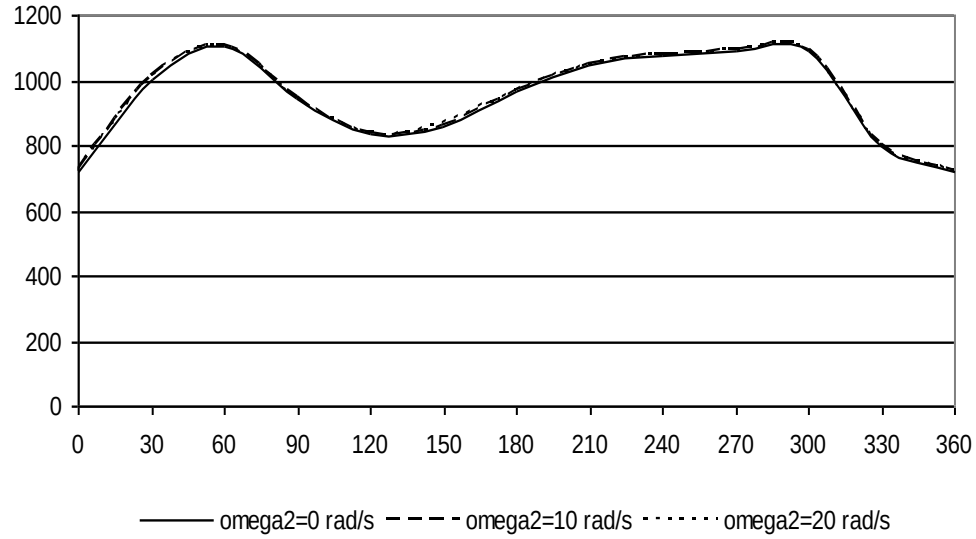


Figure 3.15. Third natural frequencies of flexible four-bar mechanism.

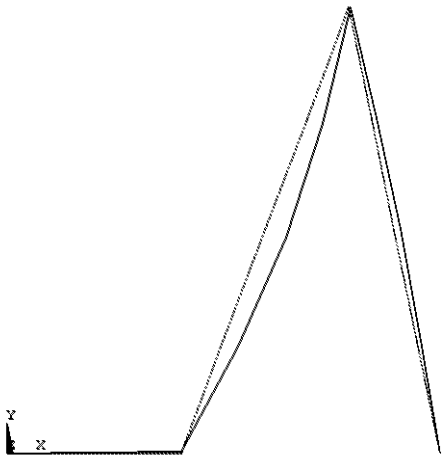


Figure 3.16. First mode shape of flexible four-bar mechanism for $\omega_2 = 10 rad/s$.

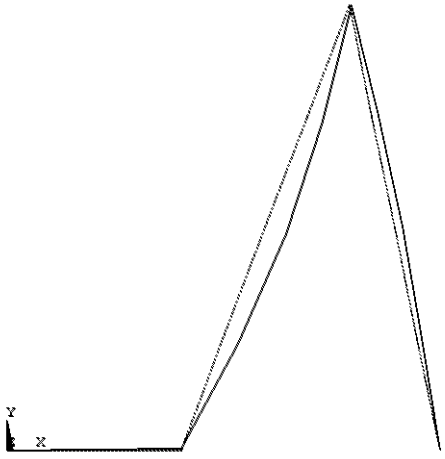


Figure 3.17. First mode shapes of flexible four-bar mechanism for $\omega_2 = 20 rad/s$.

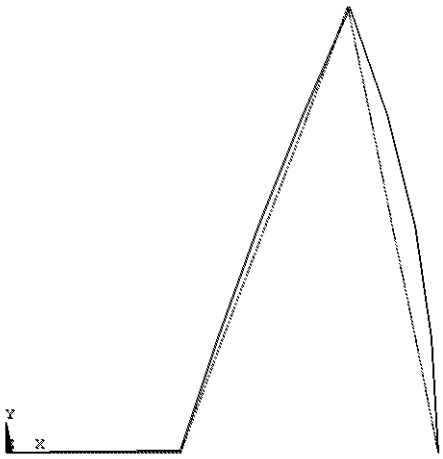

Figure 3.18. Second mode shape of flexible four-bar mechanism for $\omega_2 = 10 rad/s$.

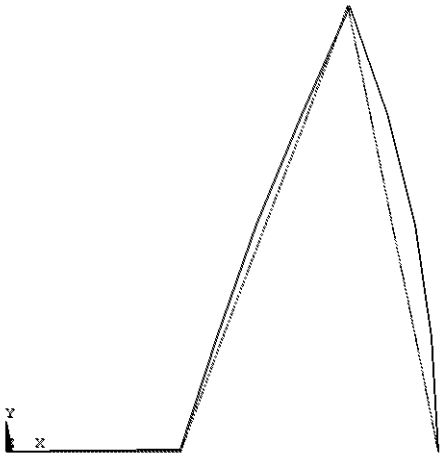

Figure 3.19. Second mode shapes of flexible four-bar mechanism for $\omega_2 = 20 rad/s$.

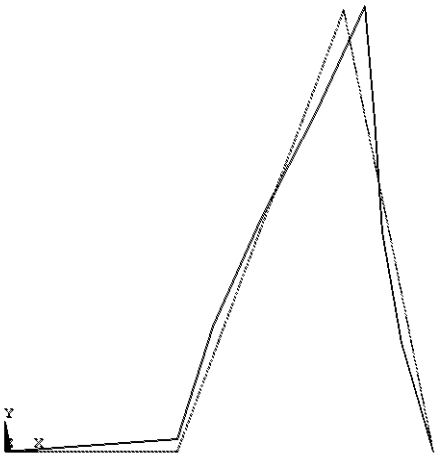

Figure 3.20. Third mode shape of flexible four-bar mechanism for $\omega_2 = 10 rad/s$.

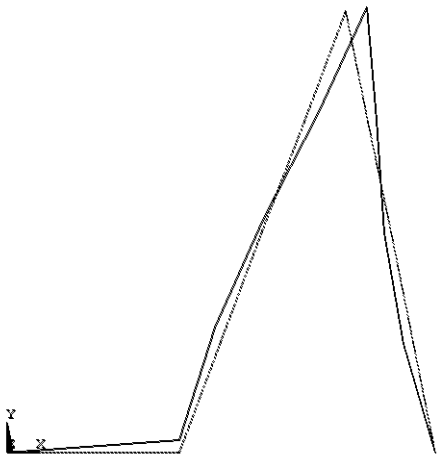

Figure 3.21. Third mode shapes of flexible four-bar mechanism for $\omega_2 = 20 rad/s$.

## 3.4. Discussion of Results

The upper and lower limits of the static natural frequencies of the flexible four-bar mechanism based on the crank angular position can be seen from the Figure 3.3. The first, second, and third mode shapes of the mechanism plotted in Figures 3.4-3.12 are consistent in each other. For example, in the first mode shapes of the mechanism for different crank angular positions, pin A has a displacement in the counterclockwise direction.

It can be seen from Figure 3.13-3.15 that the crank angular velocity is effective on the first and second dynamic natural frequencies but not on the third one. The first and second mode shapes of the mechanism plotted in Figures 3.16-3.21 are very consistent in each other, namely the links have the similar displacements for these modes.

The present results are in agreement with the results available in the literature (Yu and Xi 2003) for Figures 3.3 to 3.6 completely. On the other hand, the results given in Figures 3.13 to 3.15 are in agreement with the same literature for $30 \le \theta_2 \le 360$.

# CHAPTER 4

# CONCLUSIONS

This study presents an eigenanalysis of flexible four-bar mechanism by using finite element model conjunction with kinematic and kinetic relationships. The solution procedure based on the discrete crank positions and the discrete inertia forces applied to the nodes of the finite element model has been developed in ANSYS Parametric Design Language (APDL) to accomplish this analysis. The present results are in good agreement with the results available in literature.

# REFERENCES


Han, R.P.S. and Z.C. Zhao. 1990. Dynamics of general flexible multibody systems. *International Journal for Numerical Methods in Engineering* 30:77-97.

Karkoub, M. and A.S. Yigit. 1999. Vibration control of a four-bar mechanism with a flexible coupler link. *Journal of Sound and Vibration* 222(2):171-189.

Madenci, Erdogan and Ibrahim Guven. 2006. *The finite element method and applications in engineering using ANSYS.* Springer: The University of Arizona.

Söylemez, Eres. 1999. *Mechanisms.* METU, Publication Number:64

Tang, C.P. 2006. Lagrangian dynamic formulation of a four-bar mechanism with minimal coordinates. www.utdallas.edu/~chinpei/pdf/FourbarMinimalCoordinates.pdf

Todorov, T.S. 2002. Synthesis of four-bar mechanisms by Freudenstein–Chebyshev. *Mechanism and Machine Theory* 37:1505-1512.

Turcic, D.A. and A. Midha. 1984. Generalized Equations of Motion for the Dynamic Analysis of Elastic Mechanism Systems. *Journal of Dynamic Systems, Measurement, and Control* 106:243-248.

Turcic, D.A. and A. Midha. 1984. Dynamic Analysis of Elastic Mechanism Systems. Part I: Applications. *Journal of Dynamic Systems, Measurement, and Control* 106:249-254.

Turcic, D.A., A. Midha, and J.R Bosnik. 1984. Dynamic Analysis of Elastic Mechanism Systems. Part II: Experimental Results. *Journal of Dynamic Systems, Measurement, and Control* 106:255-260.

Yang, K. and Y. Park. 1998. Dynamic stability analysis of a flexible four-bar mechanism and its experimental investigation. *Mechanism and Machine Theory* 33:307-320.

Yang, Z. and J.P. Sadler. 2000. On issues of elastic-rigid coupling in finite element modeling of high-speed machines. *Mechanism and Machine Theory* 35:71-82.

Yu, S.D. and F. Xi. 2003. Free vibration analysis of planar flexible mechanisms. *Journal of Mechanical Design* 125(4):764-772.

Wang, Y. 1997. Dynamics of an Elastic Four Bar Linkage Mechanism with Geometric Nonlinearities. *Nonlinear Dynamics* 14:357–375.

Zhang, J.F. and Q.Y. Xu. 2004. Research on stability of periodic elastic motion of a flexible four bar crank rocker mechanism. *Journal of Sound and Vibration* 274:39-51.